

Towards Understanding the Origin of Cosmic-Ray Positrons

Zhili Weng^{†,*}

Massachusetts Institute of Technology, Cambridge, USA

E-mail: zhili.weng@cern.ch

Precision measurements of cosmic-ray positron flux by the Alpha Magnetic Spectrometer on the International Space Station are presented based on 1.9 million positrons up to 1 TeV. The positron flux exhibits distinct and complex energy dependence. The positron flux exhibits a significant excess starting from 25.2 ± 1.8 GeV followed by a sharp drop-off above 284^{+91}_{-64} GeV. In the entire energy range, the positron flux is well described by the sum of a diffuse term associated with low energy secondary positrons produced in the collision of cosmic rays, and a new source term of high energy positrons with a finite energy cutoff. This cutoff energy of the source term is determined to be 810^{+310}_{-180} GeV with a significance of more than 4σ . These experimental data show that, at high energies, positrons predominantly originate either from dark matter collisions or from new astrophysical sources.

*37th International Cosmic Ray Conference (ICRC 2021)
July 12th – 23rd, 2021
Online – Berlin, Germany*

[†]On behalf of the AMS Collaboration

*Presenter

Studies of cosmic-ray positrons and electrons are crucial for the understanding of new physics phenomena in the universe. There has been widespread interests and various explanations [1–4] of the observed excess of high energy positrons [5]. Most of these explanations differ in their predictions for the behavior of cosmic ray positrons and electrons at high energies.

The Alpha Magnetic Spectrometer (AMS) [6] is a precision general-purpose particle physics detector on the International Space Station (ISS) for the studies of the origin of dark matter, antimatter, and cosmic rays as well as to explore new physics phenomena. In this proceeding, we present precision measurements of the positron flux by AMS.

Positrons Measurement by AMS-02

The detailed description of the AMS detector, as well as the analysis procedures for positrons, are described in detail in Ref. [6, 7] and references therein. The key detector elements used for this analysis are the transition radiation detector TRD, the time of flight counters TOF, the silicon tracker, the permanent magnet, and the electromagnetic calorimeter ECAL. The tracker has nine layers, together with the magnet, it accurately determines the particle trajectory and measures rigidity R (momentum/charge), and charge sign of cosmic rays. The maximum detectable rigidity, MDR, is 2 TV for $|Z| = 1$ particles over the 3 meters lever arm from $L1$ to $L9$. The tracker also measure the particle charge $|Z|$ The TOF measures $|Z|$ and velocity with a resolution of $\Delta\beta/\beta^2 = 4\%$. The TRD separates electron (e^-) and positron (e^+) from protons (p) using 20 layers proportional tubes. The TRD estimator Λ_{TRD} is constructed from the ratio of the log-likelihood probability of the e^\pm hypothesis to that of the p hypothesis in each layer. The ECAL has 17 radiation length. It's 3-dimensional imaging capability allows for an accurate measurement of the positron energy and of the shower shape. To identify positron from proton, an ECAL estimator Λ_{ECAL} is used to differentiate e^\pm from p by exploiting their different shower shapes. To distinguish positrons from charge confusion electrons, that is, electrons which are reconstructed in the tracker with positive rigidity, a charge confusion estimator Λ_{CC}^e is defined. This technique allows for efficient separation between positron signal and electron charge confusion background.

The combination of information from the TRD, tracker, and ECAL enables the precision identification and measurement of 1.9 million positrons from 0.5 GeV to 1 TeV. These measurements reveal distinctive properties of positron flux and provide new insights into new physics phenomena in the cosmos.

Distinctive Properties of Positron Flux

The AMS positron spectrum (defined as the flux scaled by E^3) [7] is presented in Figure 1. The spectrum exhibits complex energy dependence: it is flattening from 7.10 to 27.25 GeV (green vertical band); from 27.25 to 290 GeV the positron spectrum exhibits significant rise (orange vertical band); at ~ 290 GeV the positron spectrum reaches a maximum followed by a sharp drop-off (blue vertical band). The time variation of the flux at low energies due to solar modulation is indicated by the red band.

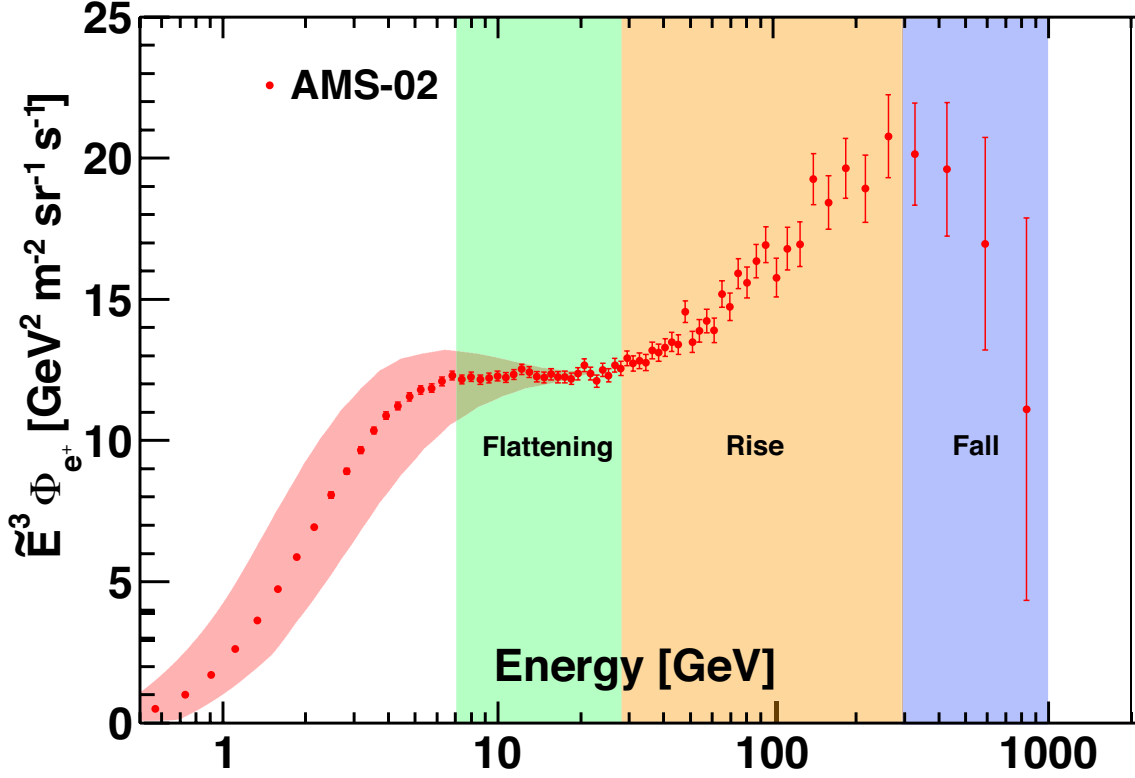


Figure 1: The positron spectrum, $\tilde{E}^3 \Phi_{e^+}$, (red data points) is shown as a function of \tilde{E} of energy. The vertical color bands indicate the energy ranges corresponding to changing behavior of the spectrum: flattening, rising(hardening), and falling(softening) spectrum.

To determine the transition energy E_0 where the positron flux changes its behavior, we use a double power-law function :

$$\Phi(E) = \begin{cases} C(E/55.58 \text{ GeV})^\gamma, & E \leq E_0; \\ C(E/55.58 \text{ GeV})^\gamma (E/E_0)^{\Delta\gamma}, & E > E_0. \end{cases} \quad (1)$$

where γ is the spectral index below E_0 and $\Delta\gamma$ is the change of the spectral index above E_0 . A fit to the data in the energy range [7.10 – 55.58] GeV yields $E_0 = 25.2 \pm 1.8$ GeV for the energy where the spectral index increases ($\Delta\gamma > 0$). The significance of this increase is established at more than 6σ . As presented in Fig. 2 a), this indicates a significant excess of the positron flux compared to the lower energy trends.

In the energy range [55.58 – 1000] GeV, the fit yields $E_0 = 284_{-64}^{+91}$ GeV for the energy of the spectral index decrease ($\Delta\gamma < 0$), as presented in Fig. 2 b). The significance of the spectral index decrease is established at more than 3σ .

Origin of High Energy Positrons

At energy starting from ~ 10 GeV, the AMS positron flux by far exceeds the contribution from secondary positrons produced from the collision of cosmic rays with the interstellar gas [8], a

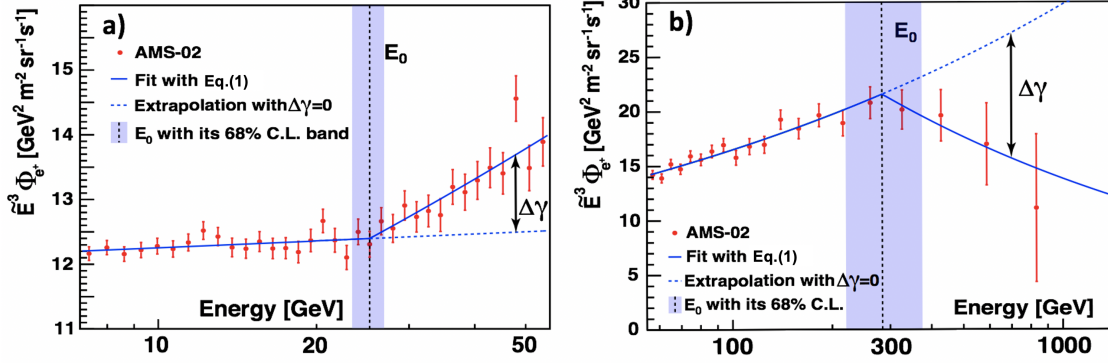


Figure 2: The double power-law fits of Eq. (1) to the positron flux in the energy ranges [7.10 – 55.58] GeV and [55.58 – 1000] GeV, respectively. The red data points are the measured positron flux scaled by \tilde{E}^3 . The fitted functions are represented by the blue lines. The vertical dashed lines and the bands correspond to E_0 and its error. The dashed blue lines are the extrapolations of the power-law below E_0 into the higher energy regions. $\Delta\gamma$ is the magnitude of the spectral index change.

primary source of positrons is needed to describe the observed positron excess. Models to explain the primary source of cosmic-ray positrons include annihilation of dark matter particles [2] and other astrophysical objects like supernova remnants or pulsars [3].

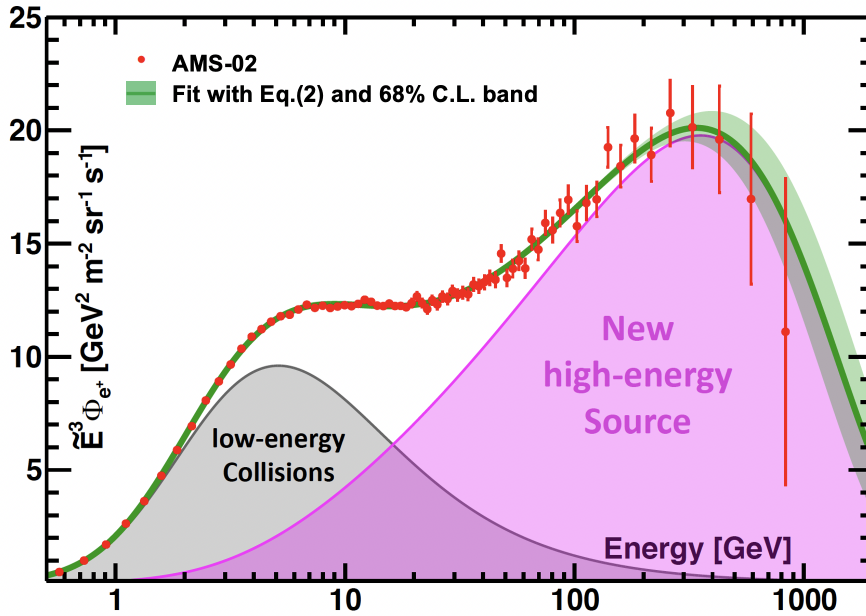


Figure 3: The fit of Eq. (2) (green line) to the positron flux in the energy range [0.5 – 1000] GeV together with the 68% C.L. interval (green band). The source term contribution is represented by the magenta area, and the diffuse term contribution by the grey area.

The accuracy of the AMS data allows for a detailed study of the properties of the new source of positrons. For example, the positron flux can be parametrized as the sum of a diffuse term and a

source term:

$$\Phi_{e^+}(E) = \frac{E^2}{\hat{E}^2} [C_d (\hat{E}/E_1)^{\gamma_d} + C_s (\hat{E}/E_2)^{\gamma_s} \exp(-\hat{E}/E_s)]. \quad (2)$$

The diffuse term is a power-law function, which describes the secondary positrons produced in the collisions of primary cosmic rays with the interstellar gas. The source term is a power-law function with an exponential cutoff, which describes the high energy part of the flux dominated by a source. The force-field approximation [9] is used to account for solar modulation effect. A detailed description of the parameters and their fitted values can be found in Ref. [7]. The fit of Eq. (2) to the measured flux yields the cutoff energy $E_s = 810_{-180}^{+310}$ GeV and $\chi^2/\text{d.o.f.} = 50/68$. The cutoff energy E_s at infinity is excluded at a significance of 4.07σ . The result of the fit is presented in Fig. 3. As seen, the diffuse term (grey filled area) dominates at low energies and gradually vanishes with increasing energy. The source term (magenta filled area) dominates the positron spectrum at high energies. These experimental data on cosmic-ray positrons shows the existence of primary source of positrons in the galaxy.

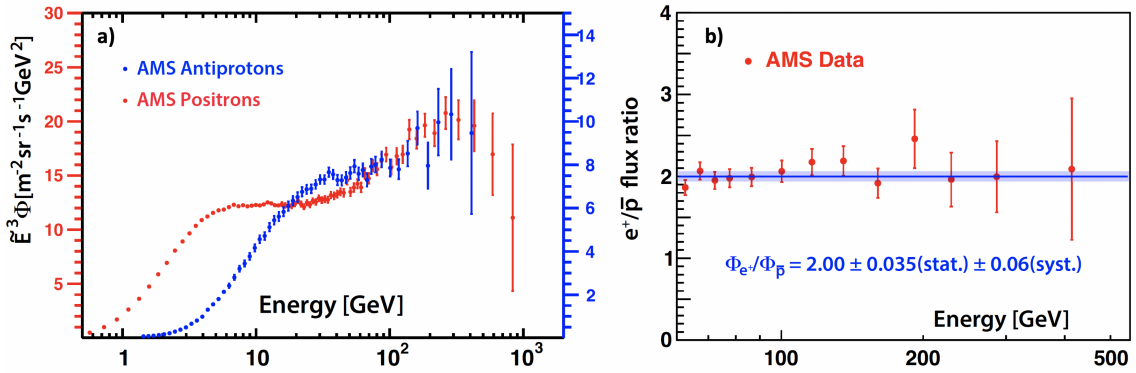


Figure 4: (a) Comparison of the AMS positron spectrum ($\tilde{E}^3 \Phi_{e^+}$, red data points, left axis) and antiproton spectrum ($\tilde{E}^3 \Phi_{\bar{p}}$, blue data points, right axis). They exhibit striking similarity at high energy. (b) The positron-to-antiproton flux ratio. In the range [60 – 525] GeV with the result of the fit with a constant value.

Positrons can be produced and accelerated from astrophysical sources like pulsars [1]. Point sources like pulsars will imprint a higher degree of anisotropy on the arrival directions of high energy positrons compared to a smooth dark matter halo. Current AMS measurements show that the incoming directions of positrons are consistent with isotropic [10]. In addition, cosmic-ray antiproton flux measured by AMS [11] is an important observation to understand the origin of cosmic-ray antimatters. Surprisingly, the AMS measurements show that the positron spectrum and the antiproton spectrum have strikingly similar behavior at high energies, as presented in Figure 4 (a). In the range [60 – 525] GeV, the positron-to-antiproton flux ratio is consistent with a constant, as presented in Figure 4 (b). The near identical behavior of positron flux and antiproton flux at a large energy range suggests a possible common source of high energy positrons and antiprotons. Antiprotons are not produced by pulsars. The continuation of AMS data taking through the life of the Space Station will improve the accuracy of these measurements and provide an important confirmation of the origin of high energy positrons.

High energy positron may originate from dark matter annihilation [2]. As an example, Figure 5 shows the comparison of the AMS data with a dark matter model based on Ref. [8, 12] with a dark

matter particle mass of 1.2 TeV. More statistics at high energies are required to verify the agreement and to understand the behavior of the positron spectrum beyond the cutoff energy.

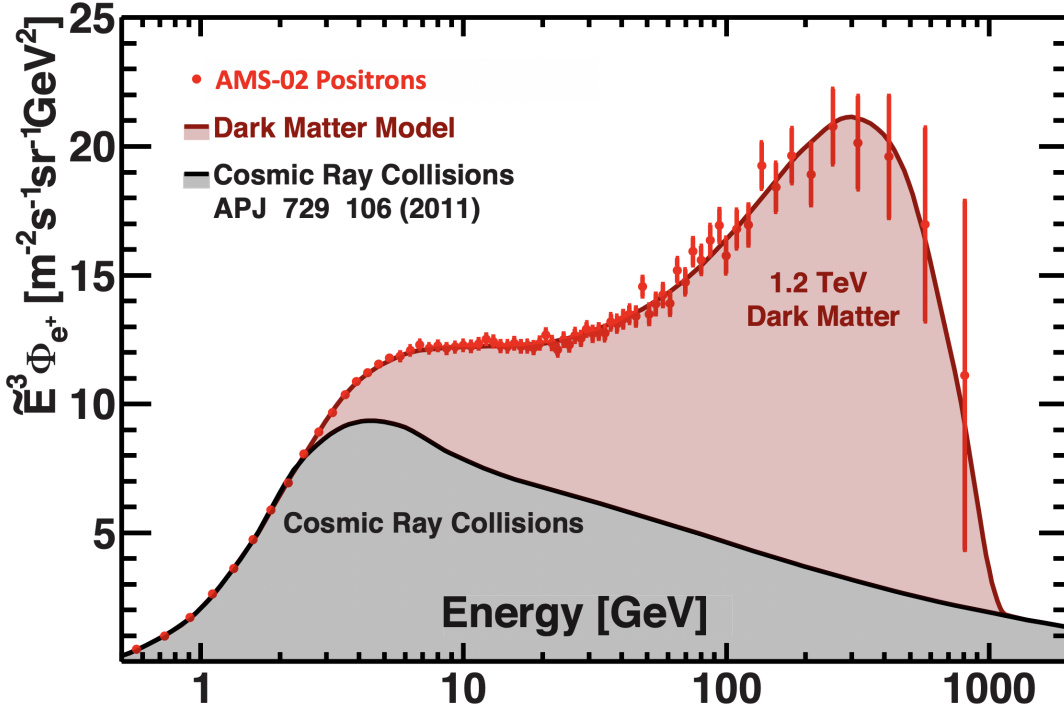


Figure 5: Comparison of the AMS data with predictions of a dark matter model based on Ref. [8, 12].

Conclusion

Precision measurement of the cosmic-ray positron flux by AMS based on 1.9 million positrons up to 1 TeV is presented. The positron flux exhibits distinct and complex energy dependence. There is a significant excess of positrons starting from 25.2 ± 1.8 GeV followed by a sharp drop-off above 284^{+91}_{-64} GeV. In the entire energy range the positron flux is well described by the sum of a diffuse term associated with low energy secondary positrons produced in the collision of cosmic rays, and a new source term of high energy positrons with a finite energy cutoff. The finite cutoff energy of the source term, E_s , is established with a significance of more than 4σ , and its value is determined to be $E_s = 810^{+310}_{-180}$ GeV. These experimental data show that at high energies, cosmic-ray positrons predominantly originate either from dark matter collisions or from new astrophysical sources.

AMS will continue to improve the accuracy and the energy reach of the measurement on positron flux so as to determine their origin at high energy.

Acknowledgement

This work has been supported by persons and institutions acknowledged in [5–7]

References

- [1] F. Donato, N. Fornengo, and P. Salati, *Phys. Rev. D* **62** 043003 (2000); M. Cirelli, R. Franceschini, and A. Strumia, *Nucl. Phys. B* **800**, 204 (2008); P. Blasi, *Phys. Rev. Lett.* **103** 051104 (2009);
- [2] M. S. Turner and F. Wilczek, *Phys. Rev. D* **42** 1001 (1990); J. Ellis, *AIP Conf. Proc.* **516**, 21 (2000); L. Bergstrom *et al.*, *Phys. Rev. Lett.* **111**, 171101 (2013);
- [3] P. D. Serpico, *Astropart. Phys.* **39-40** 2 (2012); T. Linden and S. Profumo, *Astrophys. J.* **772**, 18 (2013); P. Mertsch and S. Sarkar, *Phys. Rev. D* **90**, 061301 (2014); I. Cholis and D. Hooper, *Phys. Rev. D* **88**, 023013 (2013);
- [4] R. Cowsik, B. Burch, and T. Madziwa-Nussinov, *Astrophys. J.* **786**, 124 (2014); K. Blum, B. Katz, and E. Waxman, *Phys. Rev. Lett.* **111**, 211101 (2013).
- [5] M. Aguilar *et al.*, *Phys. Rev. Lett.* **110**, 141102 (2013); L. Accardo *et al.*, *Phys. Rev. Lett.* **113**, 121101 (2014). M. Aguilar *et al.*, *Phys. Rev. Lett.* **113**, 121102 (2014); M. Aguilar *et al.*, *Phys. Rev. Lett.* **113**, 221102 (2014).
- [6] M. Aguilar *et al.*, *Phys. Rep.*, 894, 1 (2021)
- [7] M. Aguilar *et al.*, *Phys. Rev. Lett.* **122**, 041102 (2019).
- [8] I. V. Moskalenko and A. W. Strong, *Astrophys. J.* **493**, 694 (1998); A. E. Vladimirov, S. W. Digela, G. Jóhannesson, P. F. Michelson, I. V. Moskalenko, P. L. Nolan, E. Orlando, T. A. Porter, and A. W. Strong, *Comput. Phys. Commun.* **182**, 1156 (2011). R. Trotta, G. Jóhannesson, I. Moskalenko, T. Porter, R. Ruiz de Austri, and A. Strong, *Astrophys. J.* **729**, 106 (2011).
- [9] L. Gleeson and W. Axford, *Astrophys. J.* **154**, 1011 (1968).
- [10] M. Molero *et al.*, Presented at this conference, PoS(ICRC2021)120
- [11] H.Y. Chou, Presented at this conference, PoS(ICRC2021)116
- [12] J. Kopp, *Phys. Rev. D* **88**, 076013 (2013);